Strongly screening electron capture for nuclides ^{52,53,59,60}Fe by the Shell-Model Monte Carlo method in pre-supernovae*

Jing-Jing Liu(刘晶晶)[1;1)] Qiu-He Peng(彭秋和)[2] Dong-Mei Liu(刘冬梅)[1;2)]

[1] College of Marine Science and Technology, Hainan Tropical Ocean University, Sanya 572022, China
[2] Department of Astronomy, Nanjing University, Nanjing, Jiangshu 210000, China

Abstract: The death of massive stars due to supernova explosions is a key ingredient in stellar evolution and stellar population synthesis. Electron capture (EC) plays a vital role in supernova explosions. Using the Shell-Model Monte Carlo method, based on the nuclear random phase approximation and linear response theory model for electrons, we study the strong screening EC rates of ^{52,53,59,60}Fe in pre-supernovae. The results show that the screening rates can decrease by about 18.66%. Our results may become a good foundation for future investigation of the evolution of late-type stars, supernova explosion mechanisms and numerical simulations.

Keywords: stars: supernovae, stars: evolution, physical date and processes: nuclear reactions

PACS: 24.30.-v, 26.20.Np, 26.60.Gj **DOI:** 10.1088/1674-1137/41/9/095101

1 Introduction

Supernovae not only play a critical role in the universe, but are also major sources of nucleosynthesis in stellar evolution and galactic chemical evolution. However, the driving mechanisms are still not well understood for two typical types of supernova, core-collapse (type II) and thermonuclear (type Ia) supernovae. Some studies show that electron capture (EC) and strong electron screening (SES) on medium-heavy nuclei play important roles as they lead to unstable nuclear burning and iron nucleus collapse in supernova explosions [1–3]. Thus, EC and SES have raised very interesting problems for nuclear astrophysicists in stellar evolution and nucleosynthesis. Some pioneer works on EC have been done by Fuller et al. [4, 5] (FFN), Aufderheide et al. [6, 7] (AUFD). According to the shell_model Monte Carlo method, [8–11] Langanke et al. [12, 13], and Juodagalvis et al. [14] also studied the EC reaction in detail. Liu et al. [1–3, 15–25] and Nabi et al. [26](NKK) have also discussed these issues in explosive stellar environments.

Nonetheless, there are still some challenging problems. For instance, what roles do EC and SES play in stars? How does SES influence EC rates? It is extremely important for us to accurately calculate the EC rates and screening correction for supernova explosions and numerical simulations.

^{52,53,59,60}Fe are very important nuclei in supernova explosions. Their EC rates have been widely investigated by some scholars (e.g., Refs. [4–7, 18, 20, 27, 28]). In the same environment, Liu et al. [1–3, 22] and Gutierrez et al. [29] have also discussed the weak interaction rates of ^{52,53,59,60}Fe. However, their works seem not to consider the influence of SES on EC. The SES problem has already been discussed by Bravo et al. [30] and Liu et al. [31]. The works mentioned above show that the screening corrections to EC rates in dense stars should be calculated accurately.

The effects of charge screening on nuclear physics (e.g., EC and beta decay) come at least from three factors. Firstly, the screening potential changes the electron Coulomb wave function in nuclear reactions. Secondly, the electron screening potential decreases the energy of incident electrons joining the capture reaction. Thirdly, electron screening increases the energy of the atomic nucleus (i.e., increases the single particle energy) in nuclear reactions, thus increasing the nuclear reaction rate. Finally, electron screening evidently and effectively decreases the number of higher-energy electrons, whose energy is more than the threshold of the capture reaction. Therefore, screening causes a relative increase in the re-

Received 13 February 2017, Revised 24 April 2017

* Supported by National Natural Science Foundation of China (11565020), Counterpart Foundation of Sanya (2016PT43), Special Foundation of Science and Technology Cooperation for Advanced Academy and Regional of Sanya (2016YD28), Scientific Research Staring Foundation for 515 Talented Project of Hainan Tropical Ocean University (RHDRC201701) and Natural Science Foundation of Hainan Province (114012)

1) E-mail: syjjliu68@qzu.edu.cn

2) E-mail: liudongmei72@126.com

action threshold and decrease in the capture rate, but increases the beta decay rate.

In this paper, based on the linear response theory model (LRTM) [32] and Random Phase Approximation (RPA) theory [27], by using the Shell-Model Monte Carlo (SMMC) method, we investigate the influence of SES on the EC rates for ^{52,53,59,60}Fe . We also discuss the electron capture cross section (ECCS) and the screening factors. We find the influence of SES on the rates is very significant.

Our work differs from previous works [4–7, 26] on EC. These works did not consider the influence of SES on EC. Our discussion also differs from Ref. [33], which analyzed EC using the Brink Hypothesis, based on the plasma ion ball strong screening model. They assumed that the Gamow-Teller strength distribution for excited states is the same as for the ground state, only shifted by the excitation energy of the state in their model. We analyze the effect of SES on EC by the LRTM. Our screening rates may be universal, important and helpful for research into supernova explosions and numerical simulation.

This paper is organized as follows. In the next section, we analyze the EC rates in stellar interiors with and without SES. Some numerical results and discussions are given in Section 3. Our conclusions are summarized in Section 4.

2 EC in stellar interiors

2.1 Response function and GT strength distribution

The hybrid SMMC+RPA model was proposed in Ref. [34] to compute electron capture rates on nuclei which required large model spaces. A pairing quadrupole residual interaction [35] was calculated in order to avoid the sign problem associated with using realistic interactions in SMMC studies [8–10]. At finite temperature, SMMC calculations are used to obtain occupation numbers for the various neutron and proton valence shells in the parent nucleus. SMMC is then used to calculate ECCS and rates within a Random Phase Approximation (RPA) approach with partial shell occupancies. The RPA method is explained in Ref. [36].

Based on a statistical formulation of the nuclear many-body problem, in the finite-temperature version of this approach, an observable is calculated as the canonical expectation value of a corresponding operator $\hat{A}$ by the SMMC method at a given temperature T, and is written as [8–10]

$$\hat{A}=\frac{\mathrm{Tr_A}[\hat{A}\mathrm{e}^{-\beta\hat{H}}]}{\mathrm{Tr_A}[\mathrm{e}^{-\beta\hat{H}}]}. \tag{1}$$

The problem of the shell model Hamiltonian $\hat{H}$ has been investigated in detail by Alhassid et al. [11]. When some many-body Hamiltonian $\hat{H}$ is given, a tractable expression for the imaginary time evolution operator is written as

$$\hat{U}=\exp^{-\beta\hat{H}}, \tag{2}$$

where $\beta=1/T_{\mathrm{N}}$, with T_{N} the nuclear temperature in units of MeV. $\mathrm{Tr_A}\,\hat{U}$ is the canonical partition function for A nucleons.

The SMMC method is used to calculate the response function $R_{\mathrm{A}}(\tau)$ of an operator $\hat{A}$ at an imaginary-time τ, using a spectral distribution of initial and final states $|\mathrm{i}\rangle$ and $|\mathrm{f}\rangle$ with energies E_{i} and E_{f}. $R_{\mathrm{A}}(\tau)$ is given by [12]

$$R_{\mathrm{A}}(\tau)=\frac{\sum_{\mathrm{if}}(2J_{\mathrm{i}}+1)\exp(-\beta E_{\mathrm{i}})\exp(-\tau(E_{\mathrm{f}}-E_{\mathrm{i}}))|\langle\mathrm{f}|\hat{A}|\mathrm{i}\rangle|^2}{\sum_{\mathrm{i}}(2J_{\mathrm{i}}+1)\exp(-\beta E_{\mathrm{i}})}. \tag{3}$$

Note that the total strength for the operator is given by $R(\tau=0)$. The strength distribution is given by

$$S_{\mathrm{GT^+}}(E)=\frac{\sum_{\mathrm{if}}\delta(E-E_{\mathrm{f}}+E_{\mathrm{i}})(2J_{\mathrm{i}}+1)\exp(-\beta E_{\mathrm{i}})|\langle\mathrm{f}|\hat{A}|\mathrm{i}\rangle|^2}{\sum_{\mathrm{i}}(2J_{\mathrm{i}}+1)\exp(-\beta E_{\mathrm{i}})}, \tag{4}$$

which is related to $R_{\mathrm{A}}(\tau)$ by a Laplace transform, $R_{\mathrm{A}}(\tau)=\int_{-\infty}^{\infty}S_{\mathrm{GT^+}}(E)\exp(-\tau E)\mathrm{d}E$. Note that here E is the energy transfer within the parent nucleus, and that the strength distribution $S_{\mathrm{GT^+}}(E)$ has units of MeV^{-1}.

2.2 EC process without SES

The stellar electron capture rates for the k th nucleus (Z,A) in thermal equilibrium at temperature T is given by a sum over the initial parent states i and the final daughter states f. In the case without SES, the EC rate is related to the electron capture cross-section by [14, 34]

$$\lambda_{\mathrm{ec}}^{0}(\mathrm{LJ})=\frac{1}{\pi^2\hbar^3}\sum_{\mathrm{if}}\int_{\varepsilon_0}^{\infty}p_{\mathrm{e}}^2\sigma_{\mathrm{ec}}(\varepsilon_{\mathrm{e}},\varepsilon_{\mathrm{i}},\varepsilon_{\mathrm{f}})f(\varepsilon_{\mathrm{e}},U_{\mathrm{F}},T)\mathrm{d}\varepsilon_{\mathrm{e}}, \tag{5}$$

where $\varepsilon_0=\max(Q_{\mathrm{if}},1)$. $p_{\mathrm{e}}=\sqrt{\varepsilon_{\mathrm{e}}^2-1}$ is the momentum of the incoming electron, ε_{e} is the sum of rest mass and kinetic energy of the incoming electron, U_{F} is the electron chemical potential, and T is the electron temperature. The electron Fermi-Dirac distribution is defined as $f(\varepsilon_{\mathrm{e}},U_{\mathrm{F}},T)=[1+\exp((\varepsilon_{\mathrm{e}}-U_{\mathrm{F}})/kT)]^{-1}$. $\sigma_{\mathrm{ec}}(\varepsilon_{\mathrm{e}},\varepsilon_{\mathrm{i}},\varepsilon_{\mathrm{f}})$ is the cross section for capture of an electron with energy ε_{e} from an initial proton single particle state with energy ε_{i} to a neutron single particle state with energy ε_{f}. The cross section is computed within the Random Phase Approximation.

Due to energy conservation, the electron, proton and neutron energies are related to the neutrino energy, and the Q-value for the capture reaction is given by [37]

$$Q_{\mathrm{i,f}}=\varepsilon_{\mathrm{e}}-\varepsilon_{\nu}=\varepsilon_{\mathrm{n}}-\varepsilon_{\nu}=\varepsilon_{\mathrm{f}}^{\mathrm{n}}-\varepsilon_{\mathrm{i}}^{p}, \tag{6}$$

where $\varepsilon_{\mathrm{f}}^{\mathrm{n}}-\varepsilon_{\mathrm{i}}^{\mathrm{p}}=\varepsilon_{\mathrm{if}}^{*}+\hat{\mu}+\Delta_{\mathrm{np}}$, $\hat{\mu}=\mu_{\mathrm{n}}-\mu_{\mathrm{p}}$ is the difference between neutron and proton chemical potentials in the nucleus, and $\Delta_{np}=M_n c^2-M_p c^2=1.293$ MeV, the mass difference between neutron and proton. $Q_{00}=M_f c^2-M_i c^2=\hat{\mu}+\Delta_{np}$, with M_i and M_f being the masses of the parent nucleus and the daughter nucleus respectively; ε_{if}^{*} corresponds to the excitation energies in the daughter nucleus at the states of zero temperature.

The electron chemical potential is found by inverting the expression for the lepton number density

$$n_e=\frac{8\pi}{(2\pi)^3}\int_0^\infty p_e^2(f_{-e}-f_{+e})\mathrm{d}p_e, \tag{7}$$

where $f_{-e}=[1+\exp((\varepsilon_e-U_F)/kT)]^{-1}$ and $f_{+e}=[1+\exp((\varepsilon_e+U_F)/kT)]^{-1}$ are the electron and positron distribution functions respectively, and k is the Boltzmann constant.

According to the Shell-Model Monte Carlo method, the total cross section by EC in Eq. (5) is given by [27]

$$\begin{aligned}\sigma_{ec} &= \sigma_{ec}(E_e)=\sum_{if}\frac{(2J_i+1)\exp(-\beta E_i)}{Z_A}\sigma_{fi}(E_e)\\ &= 6g_{wk}^2\int \mathrm{d}\xi(E_e-\xi)^2\frac{G_A^2}{12\pi}S_{GT^+}(\xi)F(Z,E_e)\end{aligned} \tag{8}$$

where $E_e=\varepsilon_e$ is the electron energy. S_{GT^+} is the Gamow-Teller(GT) strength distribution, which is a function of the transition energy ξ. $g_{wk}=1.1661\times10^{-5}\mathrm{GeV}^{-2}$ is the weak coupling constant and G_A is the axial vector form-factor, which at zero momentum is $G_A=1.25$. $F(Z,\varepsilon_e)$ is the Coulomb wave correction.

The pre-supernova EC rates in the case without SES is given by [12]

$$\begin{aligned}\lambda_{ec}^0(\mathrm{LJ})=&\frac{\ln2}{6163}\int_0^\infty \mathrm{d}\xi S_{GT}\frac{c^3}{(m_e c^2)^5}\\ &\times\int_{p_0}^\infty \mathrm{d}p_e p_e^2(-\xi+\varepsilon_e)^2F(Z,\varepsilon_e)f(\varepsilon_e,U_F,T)\quad(\mathrm{s}^{-1}),\end{aligned} \tag{9}$$

where ξ is the transition energy of the nucleus, and $f(\varepsilon_n,U_F,T)$ is the electron distribution function. p_0 is defined as

$$p_0=\begin{cases}\sqrt{Q_{if}^2-m_e^2c^4} & (Q_{if}<-m_e c^2)\\ 0 & (\text{otherwise}).\end{cases} \tag{10}$$

In the case without SES, we compare our results for $\lambda_{ec}^0(\mathrm{LJ})$ with those of $\lambda_{ec}^0(\mathrm{AFUD})$. The error factor C is defined as follows

$$C=\frac{(\lambda_{ec}^0(\mathrm{LJ})-\lambda_{ec}^0(\mathrm{AUFD}))}{\lambda_{ec}^0(\mathrm{LJ})}. \tag{11}$$

The RCEF plays a key role in stellar evolution and pre-supernova outbursts, and is given by

$$\dot{Y}_e^{ec}(k)=-\frac{X_k}{A_k}\lambda_k, \tag{12}$$

where X_k is the mass fraction of the k th nucleus and A_k is the mass number of the k th nucleus.

2.3 EC process with SES

The linear response theory has been discussed in detail by some authors [38, 39]. They investigated the density-functional study of hydrogen plasmas as well as the density-functional study of C, Si, and Ge metallic liquids, and found that the results of the density-functional calculations of these systems are close to the results obtained by linear response theory. They also confirmed that density functional theory as well as linear response theory satisfactorily reproduce the experimental results for Ge metallic liquid, thus proving the applicability of these theories for this system. Based on this theory, Itoh et al. [32] calculated the screening potential for relativistic degenerate electrons. We name this the linear response theory model (LRTM). Electrons are strongly degenerate in the density-temperature regime we consider. The condition is expressed as

$$T\ll T_F=5.930\times10^9\left\{\left[1+1.018\left(\frac{Z}{A}\right)^{2/3}(10\rho_7)^{2/3}\right]^{1/2}-1\right\}, \tag{13}$$

where ρ_7 is the density in units of $10^7\mathrm{g/cm}^3$, T_F is the electron Fermi temperature, and Z and A are the atomic number and mass number of the nucleus considered, respectively.

Jancovici et al. [40] calculated the static longitudinal dielectric function due to the relativistically degenerate electron liquid. When the strong screening by the relativistically degenerate electron liquid is taken into account, the electron potential energy is written as

$$V(r)=-\frac{Ze^2(2k_F)}{2k_F r}\frac{2}{\pi}\int_0^\infty\frac{\sin[(2k_F r)]q}{q\epsilon(q,0)}\mathrm{d}q, \tag{14}$$

where $\epsilon(q,0)$ is Jancovici's static longitudinal dielectric function and k_F is the electron Fermi wavenumber.

The linear response theory is a good method to calculated the screening potential for relativistic degenerate electrons [32]. A more precise screening potential in LRTM is given by

$$D=7.525\times10^{-3}Z\left(\frac{10z\rho_7}{A}\right)^{\frac{1}{3}}J(r_s,R)(\mathrm{MeV}), \tag{15}$$

where $J(r_s,R)$, r_s and R can be found in Ref. [17]. The formula (14) is valid for $10^{-5}\leq r_s\leq10^{-1}, 0\leq R\leq50$, conditions which are usually fulfilled in the pre-supernova environment.

If the electron is strongly screened, the screening energy will be high enough not to neglect in high density plasma. Its energy will decrease from ε to $\varepsilon'=\varepsilon-D$ in the decay reaction due to SES. Meanwhile, the screening causes a relative decrease in the number of high energy electrons, whose energies are higher than the threshold energy for electron capture. The threshold energy also increases from ε_0 to $\varepsilon_s=\varepsilon_0+D$. Thus the EC rate with

SES becomes

$$\lambda_{\rm ec}^{s}({\rm LJ})=\frac{\ln2}{6163}\int_{0}^{\infty}{\rm d}\xi S_{\rm GT+}\frac{c^3}{(m_{\rm e}c^2)^5}$$
$$\times\int_{\varepsilon_s}^{\infty}{\rm d}\varepsilon'\varepsilon'(\varepsilon'^2-1)^{\frac{1}{2}}(-\xi+\varepsilon')^2F(Z,\varepsilon')f(\varepsilon_{\rm e},U_{\rm F},T). \quad (16)$$

In order to understand the effect of SES on the EC, we define the screening factor C_1 as follows:

$$C_1=\frac{\lambda_{\rm ec}^{\rm s}({\rm LJ})}{\lambda_{\rm ec}^{0}({\rm LJ})}. \quad (17)$$

3 Results and disscusion

Figure 1 shows the ECCS of ^{52,53,59,60}Fe as a function of electron energy at temperature $T_9=9,11$. The ECCS increases greatly with increasing electron energy. The higher the temperature, the faster the changes in ECCS become. This is because the higher the temperature, the larger the electron energy and electron chemical potential are, so even more electrons will join in the EC process because their energy is higher than the Q-value. The minimum electron energy, which is given by the mass splitting between parent and daughter (i.e., $Q_{\rm if}$), will be a key parameter to trigger EC. At finite temperature this threshold will be lowered by the internal excitation energy. For even-even parent nuclei, the Gamow-Teller strength is centered at daughter excitation energies of the order of 2 MeV at low temperatures. Therefore, the ECCS for these parent nuclei increases dramatically within the first couple of MeV of electron energies above threshold. For odd-A nuclei, however, the Gamow-Teller distribution will peak at noticeably higher daughter excitation energies at low temperatures, so the ECCS are shifted to electron energies about 3 MeV higher than to even-even parent nuclei.

Based on RPA theory and using the SMMC method, we discuss EC in detail, especially taking account of the contribution of the GT transition. Figure 2 and 3 show the EC rates as a function of ρ_7 with and without SES. From Fig. 2, the EC rates increase by more than six orders of magnitude as the density increases (e.g. for ^{60}Fe at $T_9=3.40, Y_{\rm e}=0.47$). From Fig. 3, we find that the rates with screening are lower than those with no screening. The rates with SES may be approximately 20% lower than with no SES.

The Gamow-Teller strength distributions play an important role in the pre-collapse evolution of supernovae. The GT transition, compared with low energy transitions, may not be dominant at relatively low temperatures. At relatively high temperature and density, the GT transition strength of nuclei is distributed in the form of a centrosymmetric Gaussian function around the GT resonance point. Many electrons can therefore participate in the GT resonance transitions. Due to insufficient experimental information, the GT$^+$ transitions, which change protons into neutrons, have so far been addressed only qualitatively in pre-supernova simulations. When we assume the GT$^+$ strength to reside in a single resonance, the energy relative to the daughter ground state will be parameterized phenomenologically [4, 5]. (n, p) experiments show that the GT$^+$ strength is fragmented over many states, while the total strength is significantly quenched compared to the single particle model. The experimental information is usually obtained from (n, p) and (p, n) charge exchange reactions. However, there are no available experimental GT$^+$ strength distributions for these nuclei. Thus, we cannot give any comparison between theory and measurements.

As an example, we plot the strength distributions $S_{\rm GT+}$ as a function of excitation energy of the daughter state for ^{60}Fe nuclei. We show the calculated strength functions for GT$^+$ for the two parent states, the ground state (0^+) and first excited state (2^+) of ^{60}Fe in Figure 4. We consider and reproduce the first few low-lying levels in ^{60}Fe, which are 0, 1.1, 2.2, 2.4 MeV, corresponding to spin parities of 0^+, 2^+, 0^+, 2^+. The peak of $S_{\rm GT+}$ reaches 1.562 MeV^{-1} at 0.5 MeV for the ground state and 0.223 MeV^{-1} at 3.40 MeV for the 1st excited state for the daughter nucleus ^{60}Mn. The total GT strength distribution $B({\rm GT})_{\rm tot}$ for the ground state (0^+) and first excited state (2^+) is 9.47 MeV and 8.19 MeV, respectively. From the above discussion, by simply displacing the ground state strength distribution by the excitation energy, one can see that the GT distribution for the excited state may not be qualitatively inferred from the ground state information. In fact, an average value of the excited state distributions may be the most standard distribution, which would appear to be the one pertaining to the excited states.

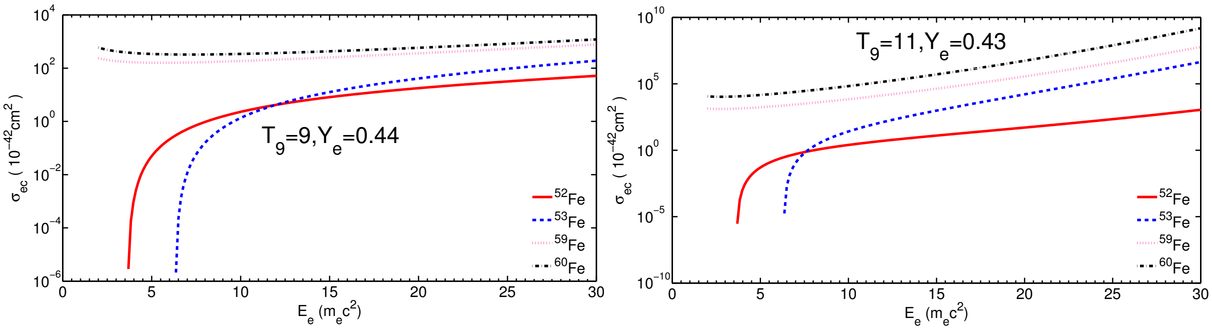

Fig. 1. (color online) ECCS for nuclides ^{52,53,59,60}Fe as a function of the electron energy at temperatures of T_9=9, Y_e=0.44 and T_9=11, Y_e=0.43 and density ρ_7=5.86.

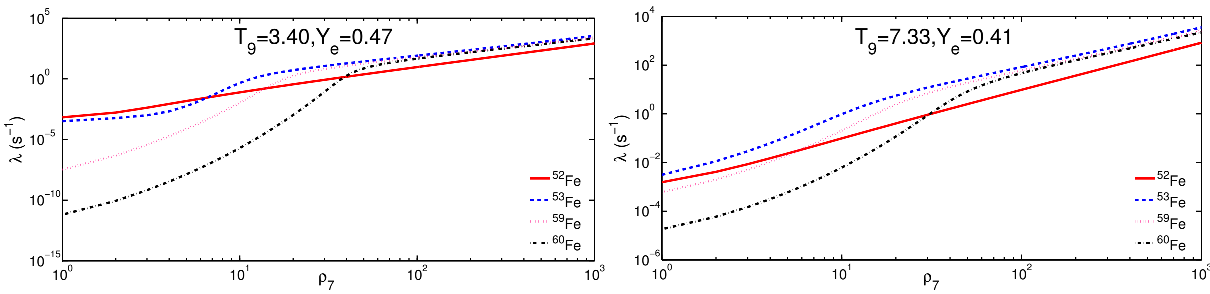

Fig. 2. (color online) Screening rates for nuclides ^{52,53,59,60}Fe as a function of density ρ_7 at temperatures of T_9= 3.40,Y_e=0.47 and T_9=7.33,Y_e=0.41.

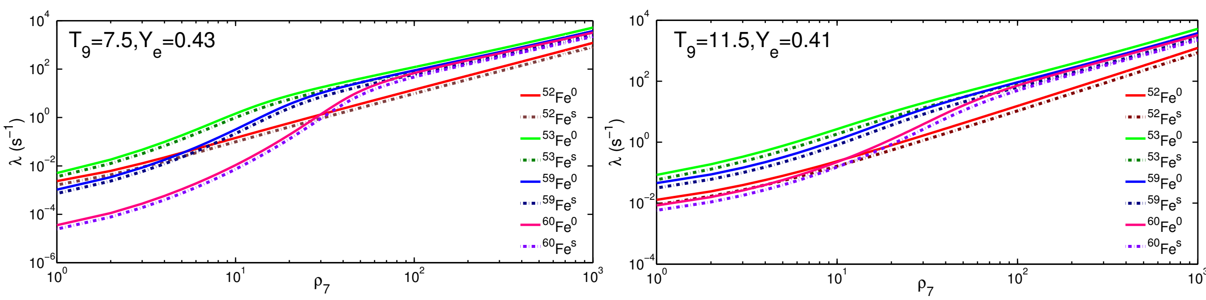

Fig. 3. (color online) EC rates with and without SES for nuclides ^{52,53,59,60}Fe as a function of density ρ_7 at temperatures of T_9=7.5,Y_e=0.43 and T_9=11.5,Y_e=0.41. The solid and dotted lines correspond to the rates without and with SES respectively.

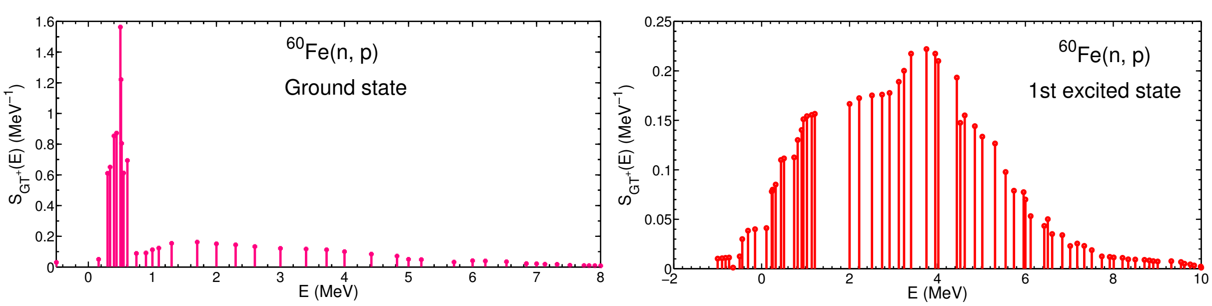

Fig. 4. (color online) Theoretical S_{GT^+} for ^{60}Fe nuclei as a function of excitation energy E at the ground state (0^+) and 1st excited state (2^+).

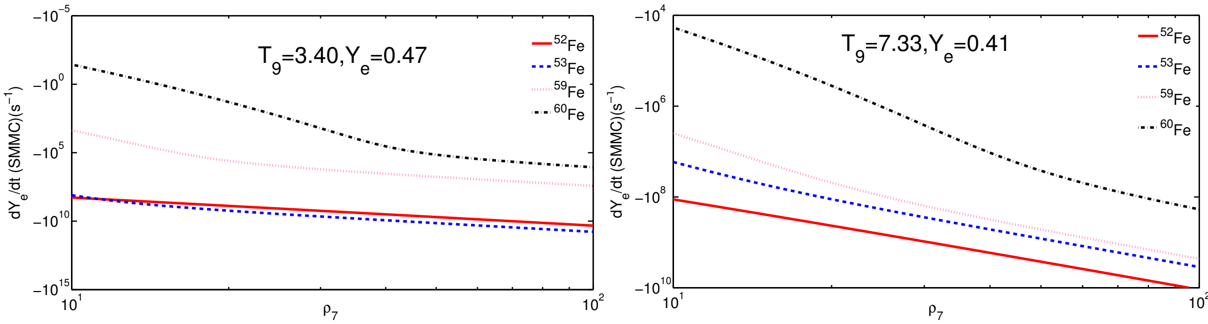

Fig. 5. (color online) RCEF due to the EC process for nuclides ^{52,53,59,60}Fe as a function of density ρ_7 at temperatures of T_9=3.40,Y_e=0.47 and T_9=7.33,Y_e=0.41.

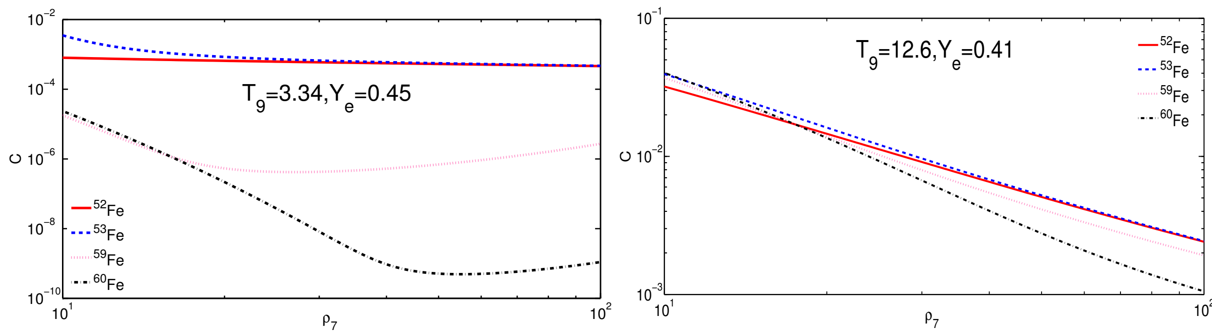

Fig. 6. (color online) The factor C for nuclides ^{52,53,59,60}Fe as a function of density ρ_7 at temperatures of T_9 = 3.34,Y_e=0.45 and T_9=12.6,Y_e=0.41.

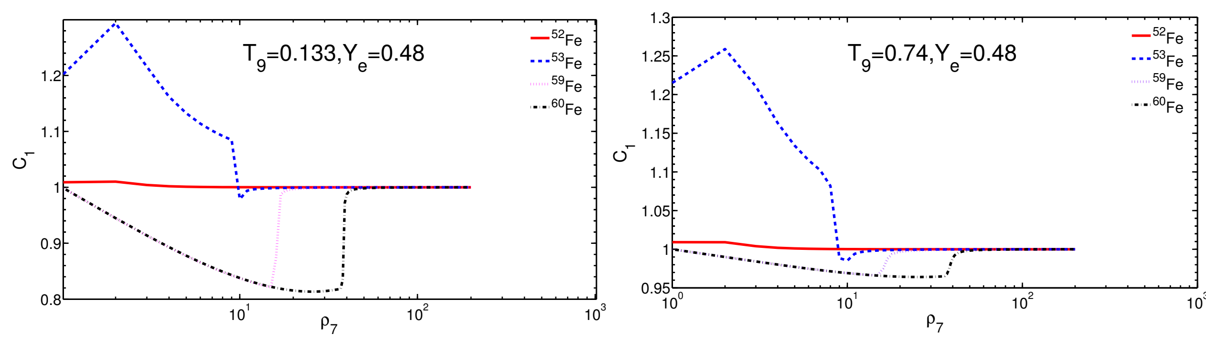

Fig. 7. (color online) The screening factor C_1 for nuclides ^{52,53,59,60}Fe as a function of density ρ_7 at temperatures of T_9=0.133,Y_e=0.48 and T_9=0.74,Y_e=0.48.

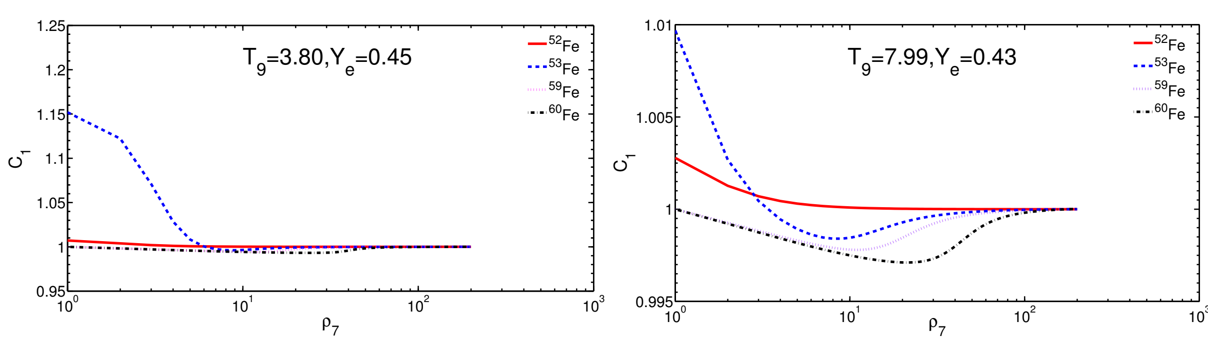

Fig. 8. (color online) The screening factor C_1 for nuclides ^{52,53,59,60}Fe as a function of density ρ_7 at temperatures of T_9=3.80,Y_e=0.45 and T_9=7.99,Y_e=0.43.

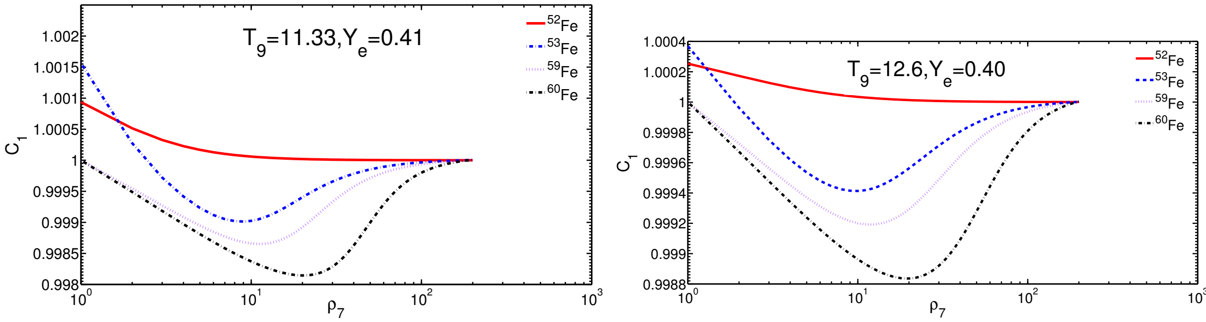

Fig. 9. (color online) The screening factor C_1 for nuclides ^{52,53,59,60}Fe as a function of density ρ_7 at temperatures of $T_9=11.33, Y_e=0.41$ and $T_9=12.6, Y_e=0.40$.

Table 1. Comparison of our calculations in the case without SES for nuclides ^{59}Fe and ^{60}Fe with those of FFN [5], AUFD [7] and NKK [26] at $\rho_7=4010, Y_e=0.41, T_9=7.33$. The ratios computed as $k_i=\frac{\lambda^0_{ec}(i)}{\lambda^0_{ec}(LJ)}$, $\lambda^0_{ec}(i)$ $(i=1,2,3)$ are the rates for FFN, AUFD, and NKK respectively in the case without SES.

nuclide	λ^0_{ec}(FFN)	λ^0_{ec}(AUFD)	λ^0_{ec}(NKK)	λ^0_{ec}(LJ)	k_1	k_2	k_3
^{59}Fe	7.20e+02	7.43e+02	2.7e+02	2.629e+02	2.739	2.816	1.027
^{60}Fe	6.73e+01	1.44e+01	3.02+01	1.749e+01	3.848	0.823	1.726

Table 2. Comparisons of our calculations for nuclides ^{59}Fe and ^{60}Fe with those of FFN [5], AUFD [7] and NKK [26] at $\rho_7=33, Y_e=0.45, T_9=4.24$. The ratios computed as $s_j=\frac{\lambda^s_{ec}(LJ)}{\lambda^0_{ec}(j)}$, $\lambda^0_{ec}(j)$ $(j=1,2,3,4)$ are the rates for FFN, AUFD, NKK, and ours respectively in the case without SES.

nuclide	λ^0_{ec}(FFN)	λ^0_{ec}(AUFD)	λ^0_{ec}(NKK)	λ^0_{ec}(LJ)	λ^s_{ec}(LJ)	s_1	s_2	s_3	s_4
^{59}Fe	6.30e−03	5.30e−03	6.20e−05	5.63e−05	5.43e−05	8.6190e−03	1.0245e−02	0.8758	0.9644
^{60}Fe	4.60e−03	1.00e−03	1.10e−05	1.08e−05	1.02e−05	2.2174e−03	1.0200e−02	0.9273	0.9444

Table 3. The minimum values of strong screening factor C_1 for some typical astronomical conditions when $1\leq\rho_7\leq200$.

	$T_9=0.133, Y_e=0.485$		$T_9=0.74, Y_e=0.481$		$T_9=3.80, Y_e=0.45$		$T_9=7.99, Y_e=0.43$	
nuclide	ρ_7	C_{min}	ρ_7	C_{min}	ρ_7	C_{min}	ρ_7	C_{min}
^{52}Fe	25	0.9986	18	0.9997	19	0.9998	41	0.9999
^{53}Fe	10	0.9788	10	0.9854	9	0.9960	8	0.9984
^{59}Fe	15	0.8220	15	0.9670	13	0.9944	12	0.9978
^{60}Fe	26	0.8134	26	0.9641	14	0.9937	21	0.9971

The RCEF is a very sensitive parameter in pre-collapse evolution of supernovae. The RCEF decreases by more than four orders of magnitude for ^{60}Fe at $T_9=7.33$ in Fig. 5. As the density and temperature increase, the electron chemical potential becomes so high that large numbers of electrons join in the EC reaction. Thus, the RCEF reduces greatly.

Based on the shell model, and the Brink Hypothesis theory, AUFD expended FFN's work and discussed the EC in detail in the case without SES. Figure 6 shows the error factor C as a function of density ρ_7. The factor C reduces greatly as the density increases. We find that our results agree well with those of AUFD at relatively high density (e.g. $\rho_7=100$) and the maximum error is within 0.35%. However, it is within 3.982% at relatively low density (e.g. $\rho_7=10$, $Y_e=0.41$, $T_9=12.6$).

As examples, comparisons of several EC rates (i.e. FFN's, AUFD's, NKK's, and ours) for ^{59}Fe and ^{60}Fe are presented in Table 1 at $\rho_7=4010$, $Y_e=0.41$, $T_9=7.33$ in the case without SES. One finds that for the even-even nuclide ^{60}Fe, the factor $k_i(i=1,2,3)$ is about 0.832, 3.848, and 1.726 respectively, corresponding to those of AUFD, FFN and NKK. However, it is 2.739, 2.816, 1.027 respectively for the odd-A nuclide ^{59}Fe.

Table 2 presents a comparison of our strong screening results with those of FFN, AUFD, NKK. From the results of s_i $(i=1, 2, 3, 4)$, one can conclude that the strong screening rates are about three and two orders magnitude lower than those of FFN and AUFD for the even-even nuclide ^{60}Fe and the odd-A nuclide ^{59}Fe, respectively. Our screening rates decrease by about 12.42% and 7.27% compared with those of NKK for ^{59}Fe and ^{60}Fe, respectively.

The screening factor C_1 is plotted as a function of

ρ_7 in Figs. 7–9. Due to SES, one finds that the rates decrease about by $\sim 18.66\%$ and $\sim 17.80\%$ in Fig. 6. The lower the temperature, the larger the effect of SES on EC rates becomes. This is because the SES mainly decreases the number of higher energy electrons, which can actively join in the EC reaction. We also find that the screening factor is nearly the same at higher density and does not depend on the temperature and density. The reason is that at higher density surroundings the electron energy is mainly determined by its Fermi energy, which is strongly decided by density. Of course, the screening of nuclear electric charges with a high electron density means a short screening length, which means a lower enhancement factor from Coulomb wave correction. However, even a relatively short electric charge screening length will not have much effect on the overall rate due to the weak interaction, which is effectively a contact potential. A bigger effect is that electrons are bound in the plasma.

Table 3 shows the numerical calculations of the minimum values of screening factor $C_{1\min}$ in detail. The EC rates of ^{52,53,59,60}Fe decrease by about $\sim$1.40%, $\sim$2.12%, $\sim$ 17.80% and $\sim$ 18.66% respectively at $T_9 = 0.133$, $Y_e = 0.485$.

Because the Q-value of EC for some neutron-rich nuclei (e.g. ^{60}Fe) has not been measured, FFN estimated it with a semiempirical atomic mass formula (see Ref. [41]). Thus, the the effective rates of FFN can be quite different. For odd-A nuclei (e.g. ^{59}Fe), FFN places the centroid of the GT strength at excitation energies which are too low (see the detailed discussions in Ref. [5]). Their rates may therefore be somewhat overestimated.

AUFD expanded FFN's works and analyzed the nuclear excited level by a simple calculation of nuclear excitation level transitions. AUFD considered that the capture rates are made up of the lower energy transition rates between the ground states and the higher energy transition rates between GT resonance states. The works of FFN and AUFD may be an oversimplification and therefore their accuracy is limited.

Using the pn-QRPA theory, NKK analyzed the nuclear excitation energy distribution. They have taken into consideration the particle emission processes, which constrain the parent excitation energies. The pn-QRPA theory calculates stronger Gamow-Teller strengths distribution from these excited states compared to those assumed using Brink' s hypothesis. However, in the GT transitions considered in their works, only low angular momentum states are considered.

The SMMC method adopts an average GT intensity distribution of electron capture and the calculated results are in good agreement with experiments, but the results for most nuclei are generally smaller than other methods, especially for some odd-A nuclei (e.g., ^{59}Fe). The charge exchange reactions (p, n) and (n, p) make it possible to observe in the weak interaction, especially for the total GT strength distribution in nuclei. For example, the EC for ^{59}Fe is dominated by the wave functions of the parent and daughter states. The total GT strength for ^{59}Fe in a full p-f shell calculation results in $B(\mathrm{GT}) = 10.1 g_A^2$ [4]. An average of the GT strength distribution is in fact obtained by the SMMC method. A reliable replication of the GT distribution in the nucleus is carried out and analysed in detail by using an amplification of the electronic shell model. Thus, the method is relatively accurate.

Summing up the above discussions, based on the theory of RPA and LRTM, using the SMMC method, we have discuss in detailed the EC rates in SES. SES has an evident effect on EC rates for different nuclei, particularly for heavier nuclides whose threshold is negative (e.g. ^{59,60}Fe) at relatively lower temperature and higher density. According to the above calculations and discussion, we can conclude that the strong screening rates can be decreased by about $\sim$18.66% with SES.

4 Conclusions

In this paper, based on RPA theory and LRTM, using the SMMC method, we have studied the EC rates of ^{52,53,59,60}Fe with and without SES. We have also discussed the influence of SES on the ECCS and the RCEF. Firstly, we find that the influence of SES on ECCS is very obvious and significant. As the electron energy increases, the ECCS increases greatly. The RCEF is a very sensitive parameter in the EC process and can decrease by more than four orders of magnitude (e.g., for ^{60}Fe at $T_9 = 7.33$). Secondly, we compare our results with those of AUFD in the case without SES. Our rates are in good agreement with those of AUFD at relatively high density (e.g., $\rho_7 = 100$) and the maximum error is within 0.35%, but is within 3.982% at relatively low density (e.g., $\rho_7 = 10, Y_e = 0.41, T_9 = 15.6$). Finally, we compare our strong screening rates with those of FFN, AUFD, and NKK. Our screening rates are about three and two orders magnitude lower than those of FFN and AUFD for ^{60}Fe and ^{59}Fe, respectively. However, the rates are decreased by about 12.42% and 7.27% compared with those of NKK for ^{59}Fe and ^{60}Fe, respectively. According to our calculations, our rates can decrease by more than $\sim$18.66% with SES.

It is generally known that EC and SES are not only among the main parameters which lead to a supernova explosion and stellar collapse, but are also relevant for simulations of the process of collapse and explosion for a massive star. The SES also strongly influences the cooling rate and evolutionary timescale. The results we derived may become a good foundation for the future investigation of late-type star evolution, supernova explosion mechanisms and numerical simulations.

The authors would like to thank the anonymous referees for carefully reading the manuscript and providing some constructive suggestions which are very helpful in improving this manuscript.

References

1 J. J. Liuand W. M. Gu, ApJS., **224**: 29 (2016)
2 J. J. Liu, MNRAS., **438**: 930 (2014)
3 J. J. Liu and D. M. Liu., Ap&SS., **361**: 246 (2016)
4 G. M. Fuller, W. A. Fowler, and M. J. Newman, ApJ., **42**: 447 (1980)
5 G. M. Fuller, W. A. Fowler, and M. J. Newman, ApJS., **48**: 279 (1982)
6 M. B. Aufderheide, G. E. Brown, T. T. S. kuo, D. B. Stout, and P. Vogel., ApJ., **362**: 241 (1990)
7 M. B. Aufderheide, I. Fushikii, S. E. Woosely, and D. H. Hartmanm, ApJS., **91**: 389 (1994)
8 M. H. Johnson and B. A. Lippmann, PhRv., **76**: 828 (1949)
9 W. E. Ormand, D. J. Dean, C. W. Johnson, et al., PhRvC., **49**: 1422 (1994)
10 S. E. Koonin, D. J. Dean, and K., Langanke, PhRep., **278**: 1 (1997)
11 Y. Alhassid, D. J. Dean, S. E. Koonin et al, PhRvL.,**72**: 613 (1994)
12 K. Langanke and G. Martinez-Pinedo, Phys. Lett. B., **436**: 19 (1998)
13 K. Langanke and G. Martinez-Pinedo, Nuclear Phys. A., **673**: 481 (2000)
14 A. Juodagalvis, K. Langanke, W. R. Hix et al, Nuclear Phys. A., **848**: 454 (2010)
15 Z. F. Gao, N. Wang, J. P. Yuan, L. Jiang, and D. L. Song, ApS&S., **332**: 129 (2011)
16 J. J. Liu and Z. Q. Luo, Chin. Phys. Lett., **16**: 1861 (2007)
17 J. J. Liu and Z. Q. Luo, Chin. Phys., **16**: 2671 (2007)
18 J. J. Liu and Z. Q. Luo, Chin. Phys., **16**: 3624 (2007)
19 J. J. Liu and Z. Q. Luo, Chin.Phys. C, **32**: 108 (2008)
20 J. J. Liu and Z. Q. Luo, Comm.Theo. Phys., **49**: 239 (2008)
21 J. J. Liu, X. P. Kang et al, Chin. Phys. C, **35**: 243 (2011)
22 J. J. Liu, Chin. Phys. C, **34**: 171 (2010)
23 J. J. Liu, Chin. Phys. C, **34**: 190 (2010)
24 J. J. Liu, Q. H, Peng, L. H. Hao et al, RAA., arXiv:1707.03504 (2017)
25 J. J. Liu, Chin. Phys. C, **37**: 51018 (2013)
26 J. Nabi and H. V. Klapdor-Kleingrothaus, EPJA, **337**: 339 (1999)
27 D. J. Dean, K. Langanke, L. Chatterjee, P. B. Radha, and M. R. Strayer, Phys. Rev. C, **58**: 536 (1998)
28 A. Heger, S. E. Woosley, G. Martinez-Pinedo, and K. Langanke, ApJ., **560**: 307 (2001)
29 J. Gutierrez, E. Garcia-Berro, I. Iben et al, ApJ., **459**: 701 (1996)
30 E. Bravo and D. Garcia-Senz, MNRAS., **307**: 984 (1999)
31 J. J. Liu, Chin. Phys. B, **19**: 099601 (2010)
32 N. Itoh, N. Tomizawa, M. Tamamura et al, ApJ., **579**: 380 (2002)
33 Z. Q. Luo and Q. H. Peng, ChA&A, **25**: 1 (2001)
34 K. Langanke, E. Kolbe, and D.J. Dean, Phys. Rev. C, **63**: 032801 (2001)
35 D.R. Bes and R.A. Sorensen, Adv. Nucl. Phys., **2**: 129 (1969)
36 E. Kolbe, K. Langanke, and P. Vogel, Nucl. Phys. A., **652**: 91 (1999)
37 J. Cooperstein, and J. Wambach, Nuclear Phys. A, **420**: 591 (1984)
38 M. W. C.Dharma-wardana, and F. Perrot, Phys. Rev. A, **26**: 2096 (1982)
39 D. Pines and P. Nozie‘res, *The Theory of Quantum Liquids* (New York: W. A. Benjamin, 1966)
40 B. Jancovici, Nuovo Cimento, **25**: 428 (1962)
41 P. A. Seeger and W. M. Howard, Nucl. Phys. A, **238**: 491 (1975)